Channel Quantization Based on the Statistical Characterization of Spatially-Correlated Fading

Fernando Domene, *Student Member, IEEE,* Gema Piñero, *Senior Member, IEEE,* Maria de Diego, *Member, IEEE,* and Alberto Gonzalez, *Senior Member, IEEE*.

Abstract

Multiuser multiple-input multiple-output (MU-MIMO) techniques, such as scheduling and precoding, have shown to improve the spectral efficiency of wireless communication systems. However, these techniques require an accurate knowledge of the channel of the different users at the transmitter. In frequency division duplex systems, this information has to be provided by the different users, motivating the research of efficient limited feedback schemes. This paper presents a novel statistical characterization of the spatial multiple-input single-output (MISO) channel. In this characterization, one antenna is selected as the reference and the channel fading experienced from this antenna is also considered as reference. The conditional probability density functions (CPDF) of the envelope and phase of the channel fading coefficients from the rest of the antennas (denoted as non-reference channel fading and non-reference antennas) are obtained given the reference one. Based on this statistical characterization, this paper proposes a channel quantization scheme that individually quantizes the channel fading coefficient of each transmit antenna that is seen by each user. The envelope and phase of the reference channel fading are quantized considering a Rayleigh distribution and a uniform distribution, respectively. The non-reference channel fading coefficients are quantized according to their respective CPDFs, which in turn depend on the spatial correlation between each channel fading and the reference channel fading. Numerical simulations have been carried out to compare the performance of the proposed conditional quantization (CQ) scheme with a polar quantization (PQ) and with a quantization based on the Karhunen-Loève (KL) transform. PQ does not consider spatial correlation, CQ needs one spatial correlation coefficient per non-reference antenna, and the KL scheme makes use of the full spatial correlation matrix. The results show that CQ achieves a lower quantization mean square error than the other two schemes in highly and moderately correlated environments. When the spatial channel model is

The authors are with the Institute of Telecommunications and Multimedia Applications (iTEAM), Universitat Politècnica de València, València, Spain (e-mail: {ferdool,gpinyero,mdediego,agonzal}@iteam.upv.es)

considered, the proposed scheme allows the spatial correlation to be successfully exploited in arrays with $N = 4$ and $N = 8$ transmit antennas for antenna separations that are lower than $d = 1.3\lambda$ and $d = 0.75\lambda$, respectively.

I. Introduction

Multiple-input multiple-output (MIMO) techniques have helped improve the spectral efficiency of wireless communication systems in the last decade [1–3]. In multiuser environments, these techniques are even more beneficial due to the multiuser diversity since they allow for the spatial multiplexing of different mobile stations (MSs), even when the MSs are not equipped with multiple antennas [4]. However, multiuser MIMO (MU-MIMO) precoding and scheduling techniques require an accurate knowledge of the channel state information (CSI) at the base station (BS) in order to achieve the expected performance.

In frequency division duplex (FDD) systems, since CSI at the BS cannot be obtained directly from the reverse link, it must be provided by the MSs, preferably through a low-rate feedback channel. The amount of feedback information depends on the system scenario and is generally larger when the channel introduces some form of disturbance, such as spatial or multiuser interference [5]. Thus, designing limited feedback schemes to reduce the amount of feedback information plays an important role in the design of multiuser communication systems.

Limited feedback schemes for MIMO and MU-MIMO systems have been extensively studied in the literature (see [5] and references therein). Many of the previous works take advantage of the correlation in the CSI in order to reduce the amount of feedback information. A multicarrier MIMO system is proposed in [6, 7], where only the beamforming vectors of a set of subcarriers are sent back by the MSs. Taking advantage of the frequency correlation, the beamforming vectors at the rest of subcarriers are obtained by spherical interpolation. In [8], the transmit beamforming vector is quantized at the receiver by using a switched codebook. An adaptive quantization framework is proposed where the codebook used for the quantization is chosen from a set of predetermined codebooks that are based on the channel statistics. Alternatively, a systematic codebook is proposed in [9], where, instead of switching the codebook, the codebook is updated through scalings and rotations using the statistical information of the channel.

In point-to-point MIMO systems, sending back the quantized beamforming matrix can be useful. However, in multiuser systems where the BS has to manage the multiuser interference

and the users do not have any information about each other, sending back the quantized per-user channel matrix can increase the flexibility in the design of scheduling and precoding. Both a user selection scheme and a precoding scheme for spatially uncorrelated channels in a MU-MIMO system are proposed in [10], where a feedback model based on channel quantization is considered. Different tradeoffs between the number of feedback bits, the number of MSs and the signal-to-noise ratio (SNR) have been derived for this system. In [11], the bandwidth is divided into resource blocks taking into account the coherence bandwidth. The channel is considered to be constant for the subcarriers within a resource block, and the design of the codebook for the channel quantization exploits the spatial and frequency correlations. A comparison between analog feedback and quantized feedback is carried out in [12], showing that quantized feedback offers a better performance. Classical uniform quantization of uncorrelated random variables is used to quantize the CSI in the time-domain. Optimal quantizers for uncorrelated Gaussian sources were obtained in [13]. These quantizers can be used for quantizing circularly-symmetric complex Gaussian sources by applying independent quantization to the real and imaginary parts, which is also known as rectangular quantization. Other authors have considered polar quantizers, where the magnitude and the phase of the complex values are independently quantized. Polar quantization has shown to slightly outperform rectangular quantization [14]. In optimal and uniform polar quantizers, the phase is quantized using an average of 1.52 and 1.47 bits more than the magnitude.

With regard to practical MU-MIMO systems, the different transmit antennas may present spatial correlation, which can be used to further reduce the feedback overhead. The idea of transform coding is to carry out a linear transformation of the original data vector in order to remove redundancy and perform the quantization over uncorrelated data [15]. The Karhunen-Loève (KL) transform is applied before channel quantization in [16] due to the fact that the KL transform achieves maximum decorrelation of Gaussian sources [17]. However, it requires the knowledge of the full spatial correlation matrix at the BS, which in turn has to be sent back by the MSs. Depending on the mobility and the number of antennas of the MSs, this amount of information can cause a critical feedback overhead in the system.

This paper presents the statistical characterization of the spatial downlink channel in a multiuser multiple-input single-output (MU-MISO) system assuming the Kronecker correlation model. In this characterization, one of the antennas in the array is chosen as the reference antenna and

the channel fading from this antenna is considered to be the reference channel fading. The fading from the rest of the channels (known as non-reference channel fading) is statistically characterized by the envelope and phase given the reference fading and the corresponding correlation coefficient.

In this work, we also propose a channel quantization scheme that makes use of this statistical characterization to reduce the feedback information. In the proposed scheme, the envelope and phase of the reference channel fading are quantized taking into account a Rayleigh distribution and a uniform distribution, respectively [18, 19]. For the non-reference channel fading, the quantization is performed considering the probability density functions (PDF), which in turn depend on the reference channel fading and the spatial correlation between each channel fading and the reference one. The main advantage of the proposed scheme is that instead of having to send back the entire correlation matrix, only the correlation coefficients between the reference channel fading and each of the non-reference fading coefficients need to be sent back. This approach can offer significant savings in feedback overhead. Numerical results have been obtained using the spatial channel model (SCM) from the Third Generation Partnership Project (3GPP) [20]. The results show that the proposed scheme outperforms the KL scheme and the scheme based on standard polar quantization in highly and moderately correlated scenarios. Thus, the contributions of this article can be summarized as follows:

- Statistical envelope and phase characterizations of the non-reference channel fading coefficients given the reference fading are presented from the results of [21, 22]. These characterizations, which focus on the channel quantization design, include the expressions of the raw moments needed for the codebook generation. An approximation of the phase difference distribution presented in [22] showing a lower computational complexity is also proposed.
- A channel quantization scheme that makes use of the envelope and phase statistical characterizations is presented. This scheme exploits the spatial correlation in order to reduce the feedback information. Comparisons to similar quantization schemes are shown and a discussion about the performance in terms of mean square error (MSE), complexity, and required feedback is also provided.

The paper is organized as follows. Section II presents the channel model and its statistical

characterization, including the envelope and the phase characterizations. Section III describes the proposed quantization scheme, which takes into account the statistical characterization. Simulations for the evaluation of the proposed scheme compared to other known quantization schemes are carried out in Section IV. Section V presents the conclusions.

The following notation is used throughout the paper: boldface upper-case letters denote matrices (e.g., $\mathbf{A}$); boldface lower-case letters denote vectors (e.g., $\mathbf{a}$); and italics denote scalars (e.g., a or A). Superscripts $(\cdot)^H$ and $(\cdot)^*$ stand for matrix Hermitian transpose and scalar complex conjugate, respectively. $\mathfrak{Re}\{\cdot\}$, $\mathfrak{Im}\{\cdot\}$, $|\cdot|$ and $\angle(\cdot)$ refer to the real part, the imaginary part, the absolute value, and the phase of a complex value, respectively. The Euclidean norm of a vector is denoted by $\|\cdot\|$. The sets of $m \times n$ real and complex matrices are denoted by $\mathbb{R}^{m\times n}$ and $\mathbb{C}^{m\times n}$, respectively. The scalar quantization of a value is expressed as $\hat{a} = \mathcal{Q}(a)$. The operators $\lceil\cdot\rceil$ and $\lfloor\cdot\rfloor$ map a real number to the smallest following integer or the largest previous integer, respectively. Finally, $\mathbb{E}[\cdot]$ denotes the expectation operator.

II. Statistical characterization of the spatial channel

We consider a narrowband MU-MISO FDD communication system with a single base station (BS) that simultaneously transmits to multiple mobile stations (MSs) using spatial multiplexing, as shown in Fig. 1. The BS is equipped with a uniform linear array of N antennas and the MSs have a single antenna. Each MS is assumed to obtain an error-free channel estimation and has to send back the quantized version of the estimated channel through the feedback channel since this information will be necessary for scheduling and precoding tasks at the BS. Focusing on a given MS, the received signal can be expressed as

$$y = \mathbf{h}^H\mathbf{x} + n, \tag{1}$$

where vector $\mathbf{h} = [h_1, \ldots, h_N]^H \in \mathbb{C}^{N\times 1}$ is composed of the channel fading coefficients between each antenna in the BS and the antenna in the MS, vector $\mathbf{x} \in \mathbb{C}^{N\times 1}$ represents the signal transmitted by the BS and is subject to a power constraint $\mathbb{E}[\|\mathbf{x}\|^2] \leq P_{\mathrm{T}}$, and n is the noise component at the MS, which follows a circularly-symmetric complex Gaussian distribution with zero mean and unit variance, $\mathcal{CN}(0, 1)$. Using the Kronecker correlation model, the channel vector can be expressed as [18, 23]

$$\mathbf{h} = \mathbf{C}_{\mathrm{s}}^{1/2}\mathbf{g}, \tag{2}$$

where $\mathbf{C}_{\mathrm{s}} = \mathbb{E}\left[\mathbf{h}\mathbf{h}^H\right] \in \mathbb{C}^{N\times N}$ is the spatial correlation matrix at the transmitter and $\mathbf{g} \in \mathbb{C}^{N\times 1}$ is a vector whose elements are independent and identically distributed (i.i.d.) circularly-symmetric complex Gaussian variables, with zero mean and unit variance, $\mathcal{CN}(0,1)$. Previous research [24] has shown that the Kronecker model results in poor estimates for capacity. However, this model is not used to evaluate the channel capacity, but to study the effect of the spatial correlation at the transmitter in the feedback scheme.

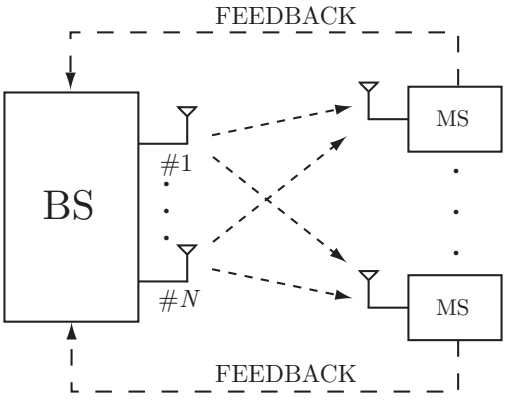

Fig. 1: System model.

In this section, we present the statistical characterization of the channel vector modeled in (2). First, a system with only $N = 2$ transmit antennas is considered; however, once the statistical characterization is stated, it is extended to the case of $N > 2$ antennas. It is important to note that, due to the separable correlation assumed in the Kronecker model [18], this analysis can be straightforwardly extended when the MSs have multiple antennas and the correlation is also present at the receiver. Let $\mathbf{g} = [g_1, g_2]^T$ be a vector with i.i.d. elements, as stated in (2), and let $\mathbf{C}_{\mathrm{s}}$ be the spatial correlation matrix at the transmitter, given by

$$\mathbf{C}_{\mathrm{s}} = \begin{bmatrix} 1 & \rho^* \\ \rho & 1 \end{bmatrix}. \tag{3}$$

Following (2) and (3), the elements of vector $\mathbf{h}$ can be expressed as

$$h_1 = k_1 g_1 + k_2^* g_2 \tag{4}$$

$$h_2 = k_2 g_1 + k_1 g_2, \tag{5}$$

where k_1 and k_2 are given by

$$k_1 = \frac{\sqrt{1+|\rho|}+\sqrt{1-|\rho|}}{2} \in \mathbb{R}^+ \tag{6}$$

$$k_2 = \frac{\rho(\sqrt{1+|\rho|}-\sqrt{1-|\rho|})}{2|\rho|} \in \mathbb{C}. \tag{7}$$

It can be noted that, for arbitrary correlated channels, $k_1^2+|k_2|^2 = 1$. For uncorrelated channels ($|\rho| = 0$), the previous equations become $k_1 = 1$ and $\lim_{|\rho|\to 0} k_2 = 0$, while for highly correlated channels ($|\rho| \approx 1$), $k_1 \approx |k_2| \approx 1/\sqrt{(2)}$. Thus, since h_1 and h_2 are a linear combination of i.i.d. $\mathcal{CN}(0,1)$ random variables, they will also show a $\mathcal{CN}(0,1)$ distribution. The real and imaginary parts of h_1 and h_2 have equal power given by

$$\mathbb{E}\left[(\mathfrak{Re}\{h_1\})^2\right] = \mathbb{E}\left[(\mathfrak{Im}\{h_1\})^2\right] = \mathbb{E}\left[(\mathfrak{Re}\{h_2\})^2\right] = \mathbb{E}\left[(\mathfrak{Im}\{h_2\})^2\right] = \frac{k_1^2+|k_2|^2}{2} = \frac{1}{2}. \tag{8}$$

The covariances between the real and imaginary parts of h_1 and h_2 are given by the following relationships:

$$\mathbb{E}\left[\mathfrak{Re}\{h_1\}\mathfrak{Im}\{h_1\}\right] = \mathbb{E}\left[\mathfrak{Re}\{h_2\}\mathfrak{Im}\{h_2\}\right] = 0 \tag{9}$$

$$\mathbb{E}\left[\mathfrak{Re}\{h_1\}\mathfrak{Re}\{h_2\}\right] = \mathbb{E}\left[\mathfrak{Im}\{h_1\}\mathfrak{Im}\{h_2\}\right] = k_1\mathfrak{Re}\{k_2\} = \frac{\mathfrak{Re}\{\rho\}}{2} \tag{10}$$

$$\mathbb{E}\left[\mathfrak{Re}\{h_1\}\mathfrak{Im}\{h_2\}\right] = -\mathbb{E}\left[\mathfrak{Im}\{h_1\}\mathfrak{Re}\{h_2\}\right] = k_1\mathfrak{Im}\{k_2\} = \frac{\mathfrak{Im}\{\rho\}}{2}. \tag{11}$$

A. Envelope statistical characterization. Case $N = 2$

Let us define, without loss of generality, transmit antenna number 2 as the reference antenna and antenna number 1 as the non-reference antenna, and their corresponding reference and non-reference channel fading coefficients as $h_{\mathrm{r}} = h_2$ and $h_{\mathrm{nr}} = h_1$. The envelope of each channel shows the following Rayleigh distribution,

$$f_{r_{\mathrm{r}}}(r_{\mathrm{r}}) = \frac{r_{\mathrm{r}}}{b_{\mathrm{R}}^2}\exp(-\frac{r_{\mathrm{r}}^2}{2b_{\mathrm{R}}^2}) \tag{12}$$

$$f_{r_{\mathrm{nr}}}(r_{\mathrm{nr}}) = \frac{r_{\mathrm{nr}}}{b_{\mathrm{R}}^2}\exp(-\frac{r_{\mathrm{nr}}^2}{2b_{\mathrm{R}}^2}), \tag{13}$$

where $r_{\mathrm{r}} = |h_{\mathrm{r}}|$, $r_{\mathrm{nr}} = |h_{\mathrm{nr}}|$ and $b_{\mathrm{R}} = \sqrt{1/2}$ is the parameter of the Rayleigh distribution.

As seen [21], the joint probability distribution of the two envelopes, r_{r} and r_{nr}, can be expressed by means of the bivariate Rayleigh distribution as

$$f(r_{\mathrm{nr}}, r_{\mathrm{r}}) = \frac{r_{\mathrm{nr}}r_{\mathrm{r}}}{b_{\mathrm{R}}^4(1-|\rho|^2)}\exp\left(-\frac{r_{\mathrm{nr}}^2+r_{\mathrm{r}}^2}{2b_{\mathrm{R}}^2(1-|\rho|^2)}\right) I_0\left(\frac{r_{\mathrm{nr}}r_{\mathrm{r}}|\rho|}{b_{\mathrm{R}}^2(1-|\rho|^2)}\right), \tag{14}$$

where $I_0(\cdot)$ is the modified Bessel function of the first kind of order 0. From (12) and (14), the conditional probability density function (CPDF) of $r_{\rm nr}$ given $r_{\rm r}$ and correlation coefficient[1] ρ can be expressed as

$$f(r_{\rm nr}|r_{\rm r},\rho)=\frac{r_{\rm nr}}{b_{\rm R}^2(1-|\rho|^2)}\exp\left(-\frac{r_{\rm nr}^2+r_{\rm r}^2|\rho|^2}{2b_{\rm R}^2(1-|\rho|^2)}\right)I_0\left(\frac{r_{\rm nr}r_{\rm r}|\rho|}{b_{\rm R}^2(1-|\rho|^2)}\right). \tag{15}$$

Fig. 2 shows the analytical CPDF described by (15) and the empirical results obtained through Monte Carlo simulations with 10^6 channel realizations for different values of reference fading envelopes, $r_{\rm r}$, and a fixed value of $|\rho|=0.9$. The Rayleigh PDF shown in (13) is denoted as Analytical Rayleigh. It can be observed that the CPDFs of the non-reference fading envelope are located approximately close to the value of the reference due to the high correlation.

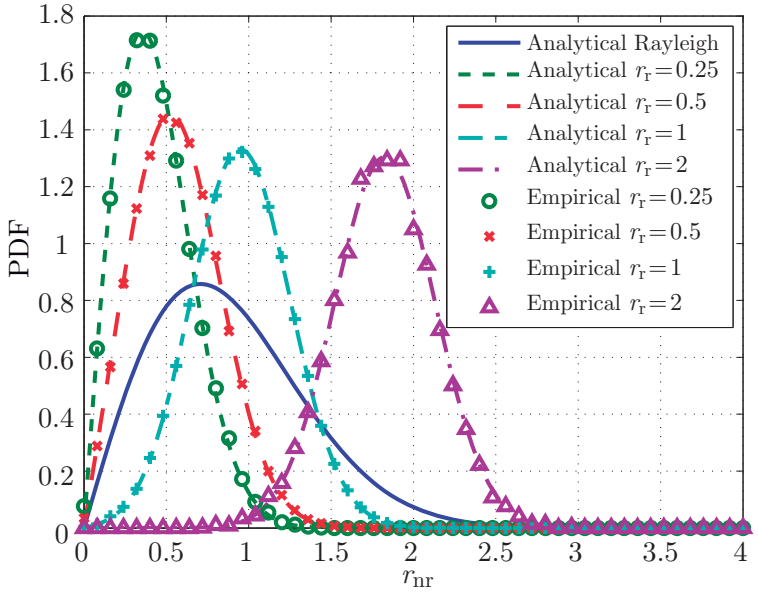

Fig. 2: Conditional probability density function of (15) for different envelope values of the reference channel fading, $r_{\rm r}$, and a fixed value of $|\rho|=0.9$.

Fig. 3 shows the analytical CPDF of (15) and the empirical results obtained through Monte Carlo simulations with 10^6 channel realizations for a fixed value of $r_{\rm r}=2$ and different values of the correlation coefficient magnitude, $|\rho|$. In this figure, it can be observed that, as the correlation

[1]In (15), we include the correlation coefficient as a parameter, $f(r_{\rm nr}|r_{\rm r},\rho)$, to explicitly note the dependence of the CPDF on ρ.

increases, the PDFs become narrower and closer to the value of the reference fading envelope. It is also important to note that (15) is equivalent to (13) for uncorrelated antennas ($|\rho| = 0$).

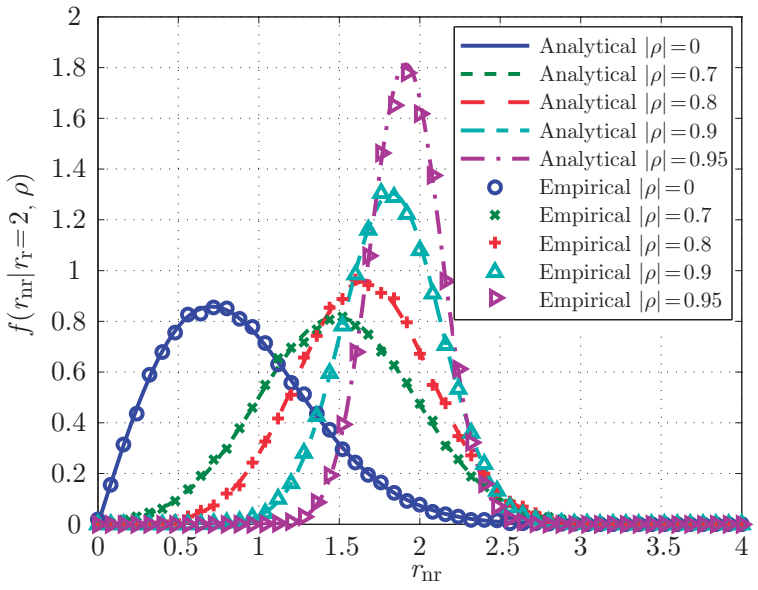

Fig. 3: Conditional probability density function of (15) for a fixed value of $r_{\rm r} = 2$ and different values of the correlation coefficient, $|\rho|$.

Expressing the modified Bessel function of the first kind of order 0, $I_0(x)$, through its Taylor series expansion around $x = 0$ [25, Sec. 9], the nth moment of $f(r_{\rm nr}|r_{\rm r},\rho)$ for a given $r_{\rm r}$ and ρ can be calculated as

$$m_n = \int_0^\infty r_{\rm nr}^n f(r_{\rm nr}|r_{\rm r},\rho)\mathrm{d}r_{\rm nr} = \exp\left(\frac{-C}{A}\right)\sum_{k=0}^{\infty}\frac{C^k\Gamma\left(k+\frac{n}{2}+1\right)}{A^{k-\frac{n}{2}}(k!)^2}, \tag{16}$$

where $A = 2b_{\rm R}^2(1-|\rho|^2)$, $C = r_{\rm r}^2|\rho|^2$, and $\Gamma(\cdot)$ is the Gamma function [25, Sec. 6]. The integral in (16) has been calculated in the Appendix within an arbitrary interval $[a, b]$, and its result can be directly applied to interval $[0, \infty]$.

As can be seen in (16), the closed expressions of the mean and variance of the PDFs cannot be easily simplified. From Fig. 2, it becomes apparent that the variance of the PDF does not significantly change with the reference fading, $r_{\rm r}$. However, Fig. 3 shows that the variance of the non-reference fading decreases and the mean value tends to get closer to the reference fading, $r_{\rm r}$, as the value of the correlation coefficient increases.

B. Phase statistical characterization. Case $N = 2$

The phase of a channel fading follows a uniform distribution in the half-open interval $[-\pi, \pi)$, and its PDF can be expressed as [26]

$$f_{\theta_{\rm r}}(\theta_{\rm r}) = f_{\theta_{\rm nr}}(\theta_{\rm nr}) = \begin{cases} \frac{1}{2\pi}, & -\pi \leq \theta < \pi \\ 0, & \text{otherwise} \end{cases} \tag{17}$$

where $\theta_{\rm r} = \angle h_{\rm r}$, $\theta_{\rm nr} = \angle h_{\rm nr}$, and θ generically denotes either $\theta_{\rm r}$ or $\theta_{\rm nr}$.

Equations (4) and (5) show that the joint probability distribution of the phases, $\theta_{\rm r}$ and $\theta_{\rm nr}$, cannot be easily calculated, and, to our knowledge, no previous work relating to the statistics of the two phases can be found in the literature. However, considering a high correlation environment with $|\rho| \approx 1$, k_2 can be written as

$$k_2 \approx e^{j\theta_\rho} k_1, \tag{18}$$

where $\theta_\rho = \angle \rho$. By substituting (18) into (4) and (5), $h_{\rm nr}$ can be written as a function of $h_{\rm r}$ expressed as $h_{\rm nr} \approx e^{-j\theta_\rho} h_{\rm r}$. Thus, the relation between the two phases is given by

$$\theta_{\rm nr} \approx \theta_{\rm r} - \theta_\rho. \tag{19}$$

This approximation holds for highly correlated channels, but it includes an error that increases as the correlation decreases. In order to evaluate the error of this approximation, we define the phase deviation as

$$\Delta = \theta_{\rm nr} - (\theta_{\rm r} - \theta_\rho). \tag{20}$$

The distribution of the phase deviation Δ has been obtained in [22]. In our case, the PDF of the phase deviation can be expressed as[2]

$$f_\Delta(\Delta, \rho) = \frac{2(1-|\rho|^2)}{3\pi(1-|\rho|\cos\Delta)^2}\ {}_2F_1\left(2, \frac{1}{2}; \frac{5}{2}; -\frac{1+|\rho|\cos\Delta}{1-|\rho|\cos\Delta}\right), \tag{21}$$

where ${}_2F_1(\cdot,\cdot;\cdot;\cdot)$ is the Gaussian hypergeometric function [25, Sec. 15].

Fig. 4 shows the analytical PDF (21) and the empirical results obtained through a Monte Carlo simulation with 10^4 channel realizations for different values of the correlation magnitude, $|\rho|$. It can be noted that, as the correlation coefficient decreases, this PDF tends to exhibit a uniform distribution, as observed in (17). On the other hand, its variance decreases as the correlation coefficient increases.

[2]In (21), the correlation coefficient is included as a parameter, $f_\Delta(\Delta, \rho)$, to explicitly note the dependence of the PDF on ρ.

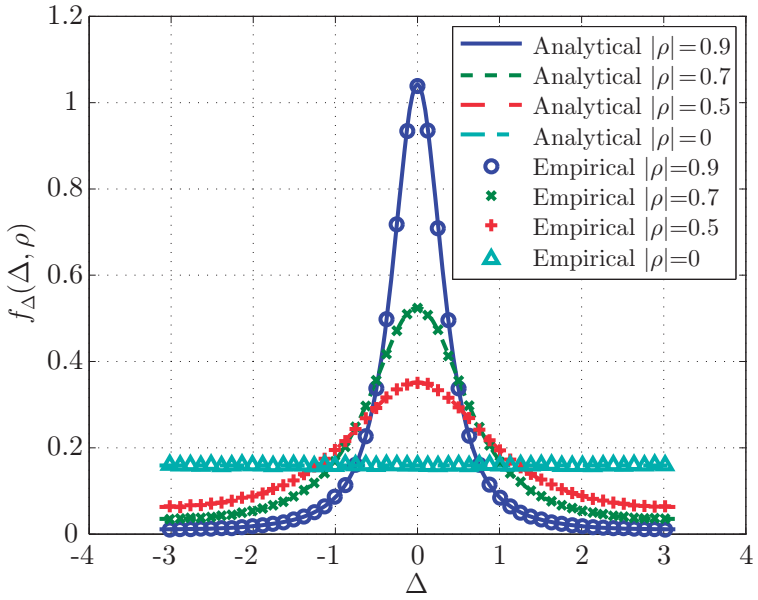

Fig. 4: Probability density function of Δ in (21) for different values of the correlation coefficient, $|\rho|$.

C. *Envelope and phase characterization for* $N > 2$

The previous characterization can be extended to a system with a linear array of $N > 2$ transmit antennas. First, an antenna is selected as a reference. The envelope and phase of the fading of the reference antenna are characterized by (12) and (17), respectively. With regard to the $N-1$ non-reference antennas, the envelope and phase of the nth non-reference channel fading are expressed as $r_{\mathrm{nr}}^{(n)}$ and $\theta_{\mathrm{nr}}^{(n)}$, respectively. The envelope and phase are characterized by their own channel fading, the correlation coefficient of the nth non-reference antenna with respect to the reference antenna, ρ_n, and the reference channel fading. Finally, (15) defines the statistical characterization of the non-reference fading envelope, $r_{\mathrm{nr}}^{(n)}$, and (21) defines the corresponding function of its phase deviation, $\Delta^{(n)}$.

III. Proposed quantization scheme

In this section, we make use of the statistical characterization discussed in Section II to propose a quantization scheme for a system with an arbitrary number of transmit antennas, N. Uniform polar quantization has been considered in the proposed scheme. The choice of uniform quantization is motivated by a lower complexity with respect to non-uniform quantization in

the codebook generation task, while the choice of polar quantization is because the statistical characterization of the channel has been obtained in terms of the envelope and phase of the channel fading coefficients. The steps for the quantization scheme are summarized in Table I. It is important to note that these steps are performed by the different MSs independently of each other.

First, a transmit antenna is chosen as a reference. In order to obtain a better quantization performance, the following heuristic formula for the selection of the reference antenna could be used:

$$N_{\mathrm{r}} = \arg\max_{N'_{\mathrm{r}}} \sum_{\substack{n=1 \\ n \neq N'_{\mathrm{r}}}}^{N} |\rho_{n,N'_{\mathrm{r}}}|, \quad 1 \leq N'_{\mathrm{r}} \leq N, \tag{22}$$

where N_{r} is the reference antenna and $\rho_{n,N'_{\mathrm{r}}}$ is the correlation coefficient between the nth and the N'_{r}th antennas. With this strategy, the selected antenna presents the highest cumulative correlation between itself and the rest of the antennas. A large correlation value provides a lower quantization error as can be inferred from Figs. 3 and 4. The fading experienced from this antenna is denoted as the reference channel fading. The channel fading coefficients from the rest of the antennas are denoted as non-reference channel fading.

The envelope and the phase of the reference channel fading (whose PDFs are given in (12) and (17), respectively) are quantized using uniform polar quantization ((A.1) and (A.2) in Table I). The non-reference channel fading coefficients are quantized taking advantage of their correlation with the reference channel fading, which is assumed to be known at both receiver and transmitter. Rows (A.3) and (A.4) in Table I show the quantization of the nth non-reference fading. The envelope quantization process considers the CPDF seen in (15). It is important to note that the CPDF uses the quantized version $\hat{r}_{\mathrm{r}}$ to quantize $r_{\mathrm{nr}}^{(n)}$, since this parameter is the one that will be available at the BS. In the phase quantization process, the phase deviation $\Delta^{(n)} = \theta_{\mathrm{nr}}^{(n)} - (\hat{\theta}_{\mathrm{r}} - \theta_{\rho_n})$ is quantized instead of quantizing $\theta_{\mathrm{nr}}^{(n)}$, since $\hat{\theta}_{\mathrm{r}}$ and θ_{ρ_n} are known by the BS. Note that, we use the PDF depicted in (33) instead of the PDF depicted in (21). This will be discussed in Section III-B. Also note that the notation for the number of bits used in the quantization of each parameter has also been included in Table I, and will be defined in Section III-D.

At the BS, the reference fading can be easily reconstructed from its quantized envelope and phase ((B.1) in Table I). The non-reference fading coefficients, $\hat{h}_{\mathrm{nr}}^{(n)}$, can be calculated using (B.2) in Table I given the relationship of the phases shown in (20).

TABLE I: Proposed quantization scheme

A.- MS: channel quantization

	Quantized value	PDF considered	Quantization bits	
1.-	$\hat{r}_{\mathrm{r}}$	(12)	$B_{M_{\mathrm{r}}}$	(A.1)
2.-	$\hat{\theta}_{\mathrm{r}}$	(17)	$B_{P_{\mathrm{r}}}$	(A.2)
3.-	$\hat{r}_{\mathrm{nr}}^{(n)}$	(15)	$B_{M_{\mathrm{nr},n}}$	(A.3)
4.-	$\hat{\Delta}^{(n)}$	(33)	$B_{P_{\mathrm{nr},n}}$	(A.4)

B.- BS: channel reconstruction

1.- $\hat{h}_{\mathrm{r}} = \hat{r}_{\mathrm{r}} \exp\left(j\hat{\theta}_{\mathrm{r}}\right)$ (B.1)

2.- $\hat{h}_{\mathrm{nr}}^{(n)} = \hat{r}_{\mathrm{nr}}^{(n)} \exp\left(j(\hat{\Delta}^{(n)} + \hat{\theta}_{\mathrm{r}} - \theta_{\rho_n})\right)$ (B.2)

A. Codebook generation for the reference channel fading

Uniform polar quantization is used to quantize the reference channel fading. The decision thresholds and the output values for the envelope ($r_{\mathrm{r},m}$, $\hat{r}_{\mathrm{r},m}$) and the phase ($\theta_{\mathrm{r},p}$, $\hat{\theta}_{\mathrm{r},p}$) of the reference channel fading have been obtained in [14] and are given by:

$$r_{\mathrm{r},m} = m d_r \qquad m = 1, \ldots, M_{\mathrm{r}} - 1 \tag{23}$$

$$\hat{r}_{\mathrm{r},m} = (m - 1/2) d_r \qquad m = 1, \ldots, M_{\mathrm{r}} \tag{24}$$

$$\theta_{\mathrm{r},p} = p d_\theta - \pi \qquad p = 1, \ldots, P_{\mathrm{r}} - 1 \tag{25}$$

$$\hat{\theta}_{\mathrm{r},p} = (p - 1/2) d_\theta - \pi \qquad p = 1, \ldots, P_{\mathrm{r}} \tag{26}$$

where $r_0 = 0$, $r_{M_{\mathrm{r}}} = \infty$, $\theta_0 = -\pi$, and $\theta_{P_{\mathrm{r}}} = \pi$. Parameters M_{r} and P_{r} are the number of quantization levels for envelope and phase, respectively, and the parameters d_r and d_θ are the interval sizes. Once M_{r} and P_{r} are fixed, the codebook is obtained by minimizing the distortion function with respect to d_r and d_θ. Since the phase is uniformly distributed, the optimal interval size for the phase is directly obtained with $d_\theta = 2\pi/P_{\mathrm{r}}$. Thus, the optimal interval size d_r can be obtained through a one-dimensional Newton-Raphson optimization technique over the distortion function [14]

$$D_{\mathrm{r}}(d_r) = \sum_{m=1}^{M_{\mathrm{r}}} \int_{r_{\mathrm{r},m-1}}^{r_{\mathrm{r},m}} \left(r_{\mathrm{r}}^2 + \hat{r}_{\mathrm{r},m}^2 - 2\mathrm{sinc}(P_{\mathrm{r}}) r_{\mathrm{r}} \hat{r}_{\mathrm{r},m}\right) f_{r_{\mathrm{r}}}(r_{\mathrm{r}}) \mathrm{d}r_{\mathrm{r}}. \tag{27}$$

In real systems, parameters such as M_{r} and P_{r} are usually considered to be power of 2 integers [5]. Thus, $B_{M_{\mathrm{r}}} = \log_2 M_{\mathrm{r}}$ and $B_{P_{\mathrm{r}}} = \log_2 P_{\mathrm{r}}$ are the number of bits dedicated to quantizing the envelope and the phase, respectively, and $B_{\mathrm{r}} = B_{M_{\mathrm{r}}} + B_{P_{\mathrm{r}}}$ is the number of bits dedicated to quantizing the reference channel fading.

B. Codebook generation for non-reference channel fading

The uniform polar quantizer shown in [14] has been used for the reference channel fading. However, Fig. 5(a) shows that a more suitable uniform quantizer for the envelope of non-reference channel fading can be obtained by including a shift parameter, d_{r0}. This parameter shifts the decision thresholds and the output values of the envelope quantizer d_{r0} units, allowing a smaller or larger first partition. The codebook for the phase of the non-reference channel fading coefficients is shown in Fig. 5(b). For the sake of clarity, we have omitted the superscript (n), which denotes the nth non-reference fading in the magnitude and phase of the channel fading coefficients and in the parameters of the quantizer, (d_{r0}, d_r, and d_Δ), since a different quantizer has to be obtained for each non-reference fading. However, the subindex n has been kept in the number of quantization levels and in the correlation coefficient as this will be needed in the study of the overall distortion and bit allocation. The partitions and the output values of the quantizer of the non-reference channel fading coefficients can be expressed as:

$$r_{\mathrm{nr},m} = d_{r0} + m d_r \qquad m = 1, \ldots, M_{\mathrm{nr},n} - 1 \tag{28}$$

$$\hat{r}_{\mathrm{nr},m} = d_{r0} + (m - 1/2) d_r \qquad m = 1, \ldots, M_{\mathrm{nr},n} \tag{29}$$

$$\Delta_p = p d_\Delta \qquad p = -\left(\frac{P_{\mathrm{nr},n}}{2} - 1\right), \ldots, \left(\frac{P_{\mathrm{nr},n}}{2} - 1\right) \tag{30}$$

$$\hat{\Delta}_p = (p - 1/2) d_\Delta \qquad p = -\left(\frac{P_{\mathrm{nr},n}}{2} - 1\right), \ldots, \frac{P_{\mathrm{nr},n}}{2} \tag{31}$$

where $M_{\mathrm{nr},n}$ and $P_{\mathrm{nr},n}$ are the number of quantization levels for the envelope and phase of the nth non-reference channel fading, respectively, and m and p are integers.

For fixed values of the number of quantization levels for envelope and phase, and omitting the quantization error of the reference fading, the distortion function for the nth non-reference channel fading, given a certain reference envelope r_{r} and the correlation coefficient between the

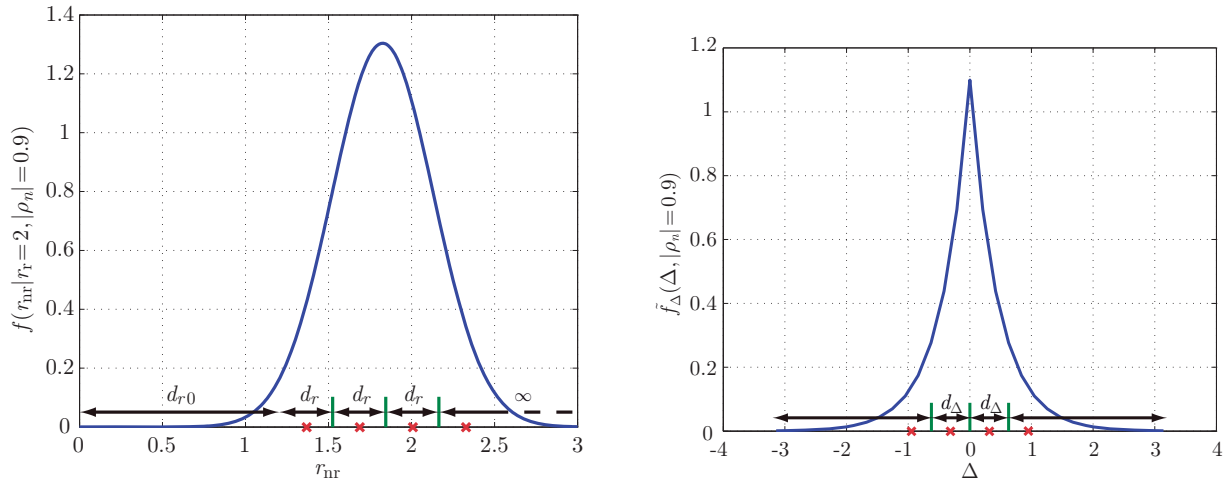

(a) Codebook for envelope quantization

(b) Codebook for phase quantization

Fig. 5: Illustrative example of parameters d_{r0}, d_r, and d_Δ for a non-reference codebook for $r_{\rm r}=2$, $|\rho_n|=0.9$, $M_{{\rm nr},n}=4$, and $P_{{\rm nr},n}=4$. The partitions and the output values are represented by green segments and red X marks, respectively.

nth non-reference channel fading and the reference one, ρ_n, can be expressed as

$$D_{\rm nr}(d_{r0},d_r,d_\Delta,\rho_n|r_{\rm r}) = \sum_{m=1}^{M_{{\rm nr},n}}\sum_{p=1}^{P_{{\rm nr},n}}\int_{r_{{\rm nr},m-1}}^{r_{{\rm nr},m}}\int_{\Delta_{p-1}}^{\Delta_p}\left|r_{\rm nr}e^{j\Delta}-\hat{r}_{{\rm nr},m}e^{j\hat{\Delta}_p}\right|^2 f(r_{\rm nr}|r_{\rm r},\rho_n)f_\Delta(\Delta,\rho_n)\mathrm{d}r_{\rm nr}\mathrm{d}\Delta, \quad (32)$$

where $\Delta=\theta_{\rm nr}-(\hat{\theta}_{\rm r}-\theta_{\rho_n})$ is the phase deviation. Likewise, $M_{{\rm nr},n}$ and $P_{{\rm nr},n}$ are considered to be power of 2 integers. Thus, $B_{M_{{\rm nr},n}}=\log_2 M_{{\rm nr},n}$, $B_{P_{{\rm nr},n}}=\log_2 P_{{\rm nr},n}$, and $B_{{\rm nr},n}=B_{M_{{\rm nr},n}}+B_{P_{{\rm nr},n}}$ are the number of bits dedicated to quantizing the envelope, the phase, and the total number of bits for the nth non-reference channel fading, respectively.

The solution for the definite integrals in (32) that involve the PDF of the phase deviation, $f_\Delta(\Delta,\rho_n)$, requires numerical integration and the evaluation of the Gaussian hypergeometric function, ${}_2F_1(\cdot,\cdot;\cdot;\cdot)$, which results in a significant computational cost. In addition, the minimization algorithm may require multiple evaluations of the distortion function at different points to obtain the optimal codebook for each non-reference channel fading. In order to avoid this highly demanding computation, we present an approximation to (21) using a truncated Laplace

distribution:

$$\tilde{f}_{\Delta}(\Delta,\rho_n)=\begin{cases}\frac{\exp\left(-|\Delta|/b_{\mathrm{L},n}\right)}{2b_{\mathrm{L},n}\left(1-\exp\left(-\pi/b_{\mathrm{L},n}\right)\right)}, & -\pi\leq\Delta<\pi\\ 0, & \text{otherwise}\end{cases} \tag{33}$$

where $b_{\mathrm{L},n}$ is the parameter of the Laplace distribution that can be accurately adjusted in terms of least square fitting for high correlation environments by

$$b_{\mathrm{L},n}^2=0.52|\rho_n|^2-2.96|\rho_n|+2.45. \tag{34}$$

This approximation allows the definite integral in (32) to be solved analytically using the results provided in the Appendix.

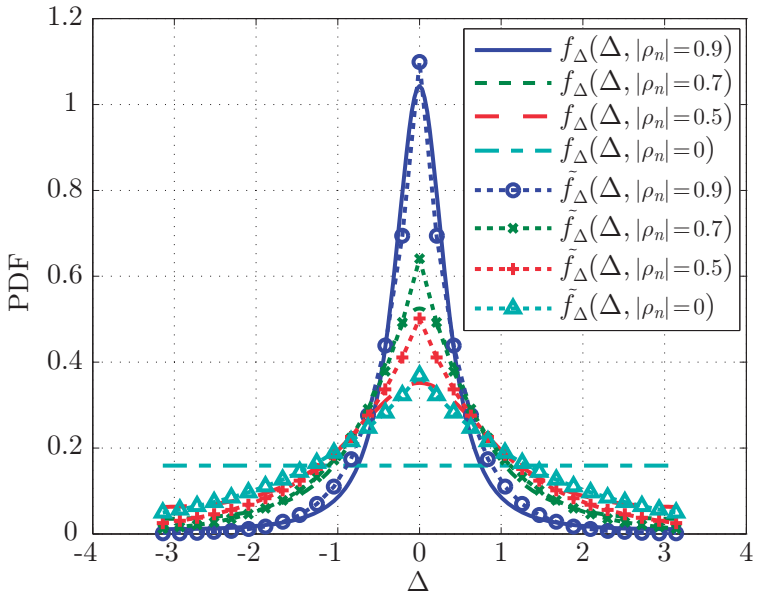

Fig. 6: Analytical PDF of the phase deviation, $f_{\Delta}(\Delta,\rho_n)$, and its approximation using the Laplace distribution, $\tilde{f}_{\Delta}(\Delta,\rho_n)$, for different values of the correlation coefficient, $|\rho_n|$.

Fig. 6 shows the analytical PDF of the phase deviation, seen in (21), and the proposed Laplace approximation, seen in (33), for different values of ρ_n. It can be observed that, as the correlation coefficient increases, the approximation is closer to the analytical PDF and it includes a higher error for small magnitudes of the correlation coefficient.

Using the proposed approximation (33) in (32), the distortion for the nth non-reference channel fading given a certain reference envelope, r_{r}, and the correlation coefficient between the nth non-

reference antenna and the reference antenna, ρ_n, can be expressed as

$$
\begin{aligned}
&D_{\mathrm{nr}}(d_{r0}, d_r, d_\Delta, \rho_n | r_{\mathrm{r}}) = \\
&\sum_{m=1}^{M_{\mathrm{nr},n}} \int_{r_{\mathrm{nr},m-1}}^{r_{\mathrm{nr},m}} r_{\mathrm{nr}}^2 f(r_{\mathrm{nr}}|r_{\mathrm{r}}, \rho_n) \mathrm{d}r_{\mathrm{nr}} + \sum_{m=1}^{M_{\mathrm{nr},n}} \hat{r}_{\mathrm{nr},m}^2 \int_{r_{\mathrm{nr},m-1}}^{r_{\mathrm{nr},m}} f(r_{\mathrm{nr}}|r_{\mathrm{r}}, \rho_n) \mathrm{d}r_{\mathrm{nr}} \\
&- 2 \sum_{m=1}^{M_{\mathrm{nr},n}} \hat{r}_{\mathrm{nr},m} \int_{r_{\mathrm{nr},m-1}}^{r_{\mathrm{nr},m}} r_{\mathrm{nr}} f(r_{\mathrm{nr}}|r_{\mathrm{r}}, \rho_n) \mathrm{d}r_{\mathrm{nr}} \sum_{p=1}^{P_{\mathrm{nr},n}} \int_{\Delta_{p-1}}^{\Delta_p} \cos(\Delta - \hat{\Delta}_p) \tilde{f}_\Delta(\Delta, \rho_n) \mathrm{d}\Delta,
\end{aligned}
\tag{35}
$$

where the first three integrals can be solved using the 2nd, 0th, and 1st moments of $f(r_{\mathrm{nr}}|r_{\mathrm{r}}, \rho_n)$, respectively, as shown in (16). The solution for the fourth integral can be found in equation (48) of the Appendix.

The convergence of the minimization of the distortion expressed in (35), which is a 3-dimension minimization problem on (d_{r0}, d_r, d_Δ), is not straightforward to analyze and is out of the scope of this paper. The Nelder-Mead simplex method can be used to minimize the distortion due to the good convergence properties that it has demonstrated in other problems and because it does not require any derivative information [27].

We carried out preliminary simulations using non-uniform codebooks and the MSE obtained has been slightly lower. Nevertheless, the convergence criterion of the minimization problem for non-uniform codebooks was not met in all cases. For this reason, we have only included the results obtained with uniform codebooks, where the convergence was achieved in all cases.

C. Overall distortion

In order to express the overall distortion, it is necessary to determine both the distortion due to the quantization of the reference channel fading and the distortion due to the quantization of the non-reference channel fading. In what follows, it is assumed that the aforementioned quantizers are always optimized for the different number of levels and that the distortion is expressed in terms of the number of quantization bits. Thus, the distortion in the reference and non-reference fading quantization, seen in (27) and (32), for different number of quantization bits is denoted as $D_{\mathrm{r}}(B_{M_{\mathrm{r}}}, B_{P_{\mathrm{r}}})$ and $D_{\mathrm{nr}}(B_{M_{\mathrm{nr},n}}, B_{P_{\mathrm{nr},n}}, \rho_n | r_{\mathrm{r}})$, respectively.

The distortion in a non-reference channel fading has been expressed in (32) and depends on the current reference channel fading and the correlation coefficient. The average distortion in the

nth non-reference channel fading for a given correlation coefficient can be expressed as

$$D_{\mathrm{nr}}(B_{M_{\mathrm{nr},n}}, B_{P_{\mathrm{nr},n}}, \rho_n) = \sum_{m=1}^{M_{\mathrm{r}}} D_{\mathrm{nr}}(B_{M_{\mathrm{nr},n}}, B_{P_{\mathrm{nr},n}}, \rho_n | \hat{r}_{\mathrm{r},m}) P(\hat{r}_{\mathrm{r},m}), \tag{36}$$

where $\hat{r}_{\mathrm{r},m}$ is the mth value in the codebook of the reference envelope and $P(\hat{r}_{\mathrm{r},m})$ is the probability of quantizing a reference envelope with the value $\hat{r}_{\mathrm{r},m}$, (i.e., the probability of the mth envelope decision interval). This probability is given by

$$P(\hat{r}_{\mathrm{r},m}) = \int_{r_{\mathrm{r},m-1}}^{r_{\mathrm{r},m}} f(r_{\mathrm{r}}) \mathrm{d}r_{\mathrm{r}} = \Gamma\left(1, \frac{r_{\mathrm{r},m-1}^2}{2b_{\mathrm{R}}^2}\right) - \Gamma\left(1, \frac{r_{\mathrm{r},m}^2}{2b_{\mathrm{R}}^2}\right) \ , \tag{37}$$

where $\Gamma(s, x)$ denotes the upper incomplete Gamma function [25, Sec. 6]. Thus, the distortion over the whole channel vector can be expressed as

$$D(B_{M_{\mathrm{r}}}, B_{P_{\mathrm{r}}}, \mathbf{b}_{M_{\mathrm{nr}}}, \mathbf{b}_{P_{\mathrm{nr}}}, \boldsymbol{\rho}) = D_{\mathrm{r}}(B_{M_{\mathrm{r}}}, B_{P_{\mathrm{r}}}) + \sum_{n \in \mathcal{S}_{\mathrm{nr}}} D_{\mathrm{nr}}(B_{M_{\mathrm{nr},n}}, B_{P_{\mathrm{nr},n}}, \rho_n), \tag{38}$$

where $\mathbf{b}_{M_{\mathrm{nr}}}$, $\mathbf{b}_{P_{\mathrm{nr}}}$, and $\boldsymbol{\rho}$ are vectors that contain $B_{M_{\mathrm{nr},n}}$, $B_{P_{\mathrm{nr},n}}$, and ρ_n for the $N-1$ non-reference channel fading coefficients and $\mathcal{S}_{\mathrm{nr}}$ is the set of the $N-1$ non-reference antennas. The number of quantization bits dedicated to quantizing the non-reference fading coefficients is given by $B_{\mathrm{nr}} = \sum_{n \in \mathcal{S}_{\mathrm{nr}}} B_{\mathrm{nr},n}$, and the total number of quantization bits is $B = B_{\mathrm{r}} + B_{\mathrm{nr}}$.

D. Bit allocation

The previous subsections have shown how to obtain the optimal codebook that minimizes the distortion in reference and non-reference channel fading. However, the solution for allocating the total amount of bits to quantize the envelopes and phases of the reference and non-reference channel fading has not been discussed yet.

The number of bits dedicated to quantizing the reference channel fading depends on the correlation between the channel fading coefficients. For uncorrelated or low-correlated environments, the best performance is obtained with an equal bit allocation per channel fading since the PDFs of the different fading coefficients are almost equal. However, as the correlation increases, a lower overall distortion can be achieved by increasing the number of bits of the reference channel fading, since this value will be used for the quantization of non-reference fading coefficients and the variance of the rest of fading coefficients will be lower. In the proposed scheme, the number of quantization bits for the reference channel fading varies from $B_{\mathrm{r}} = \lceil B/N \rceil$ to $B_{\mathrm{r}} = \lceil B/N \rceil + 3$,

depending on the correlation. Therefore, the optimal bit allocation is obtained from pre-calculated tables.

For the envelope and phase quantization of the reference channel fading, as shown in [14], the average ratio between the number of levels of the phase and the magnitude quantizers for the minimum distortion is 2.77, which is equivalent to allocating 1.47 more bits to the phase than to the magnitude. Since the number of levels are assumed to be power of 2 integers, this condition can be obtained by ensuring that

$$(B_{M_{\mathrm{r}}}, B_{P_{\mathrm{r}}}) : \begin{cases} B_{P_{\mathrm{r}}} - B_{M_{\mathrm{r}}} = 1 & B_{\mathrm{r}} \text{ odd} \\ B_{P_{\mathrm{r}}} - B_{M_{\mathrm{r}}} = 2 & B_{\mathrm{r}} \text{ even} \end{cases} \tag{39}$$

We have checked that this technique obtains the minimum distortion for integer bit allocation in at least the range $3 \leq B_{\mathrm{r}} \leq 14$. Therefore, the number of bits dedicated to the reference envelope and phase can be calculated directly as follows

$$B_{M_{\mathrm{r}}} = \left\lceil \frac{B_{\mathrm{r}}}{2} \right\rceil - 1 \tag{40}$$

$$B_{P_{\mathrm{r}}} = \left\lfloor \frac{B_{\mathrm{r}}}{2} \right\rfloor + 1. \tag{41}$$

With regard to the bit allocation between the non-reference antennas, B_{nr} bits have to be allocated between the envelope and phase of the non-reference fading coefficients $B_{M_{\mathrm{nr},n}}$ and $B_{P_{\mathrm{nr},n}}$ bits, respectively, in order to minimize (38). The greedy bit allocation algorithm shown in [15] is used to perform this task. This algorithm consists of allocating one bit at a time to the most needy variable among the different envelopes and phases, where the degree of neediness is measured by the average distortion given in (36). Even though this allocation is not optimal, it yields good assignments in practice [15]. The results show that the overall distortion is minimized by dedicating more bits to those channel fading coefficients that exhibit a lower correlation with the reference coefficient, which in a linear array would be those fading coefficients whose antennas are located the farthest away from the reference one.

IV. Numerical results

In this section, we evaluate the performance of the proposed quantization scheme. In what follows, we will refer to this scheme as the conditional quantization (CQ) scheme since the quantization of the non-reference channel fading coefficients is influenced by the reference fading.

To the best of our knowledge, no previous work has proposed different PDFs that are based on the correlation coefficient in order to quantize the different channel fading coefficients. Thus, the proposed scheme is compared with a scheme that is based on polar quantization (PQ) where identical PDFs are used for all the channel fading coefficients since that scheme does not consider correlation [14], and with another scheme that is based on the KL transform [15, 16]. The greedy bit allocation algorithm is used in both of these schemes [15].

As stated in Section I, the KL scheme requires the knowledge of the entire spatial correlation matrix at the BS. Since the spatial correlation matrix exhibits a Hermitian symmetry with unit diagonal [28], it can be reconstructed at the BS by sending back the coefficients above or below the main diagonal. Therefore, the number of coefficients of the spatial correlation matrix that need to be estimated and sent back in the KL scheme is given by

$$N_{\mathrm{c,KL}} = \frac{N(N-1)}{2}, \tag{42}$$

and it increases with N^2. The CQ scheme only requires the correlation coefficients between the reference channel fading and the fading of the rest of antennas, that is,

$$N_{\mathrm{c,CQ}} = N - 1, \tag{43}$$

resulting in a linear relation between the number of coefficients and the number of antennas. Thus, the KL scheme needs to estimate and provide $N/2$ times the number of correlation coefficients sent back by the CQ scheme. Since the MSs have different spatial correlation matrices depending on their location, this information has to be fed back by every MS. In contrast, the PQ scheme does not require any correlation coefficient.

MSs must keep the spatial correlation information periodically updated. The periodicity parameter N_{pd} (in subframes) shows how often this information is updated in the LTE-Advanced standard [29]. Since one CSI reference signal is sent every subframe [30, Chap. 29], we define the parameter $L_{\mathrm{ch}} = N_{\mathrm{pd}}$ as the number of channel quantizations that can be carried out before updating the correlation information. Note that the quantization of the spatial correlation matrix entails a reduction of the feedback rate dedicated to quantizing the instantaneous channel information in systems with a fixed feedback rate.

With regard to the computational complexity of the CQ and KL schemes, the CQ directly quantizes the envelope and phase of the channel fading coefficients, while the KL must perform

a KL transform, and subsequently quantize the resulting KL coefficients. On the other hand, the CQ scheme requires the calculation of an independent codebook for each value of the correlation coefficient and each quantized value of the envelope of the reference channel fading, while the KL scheme simply scales a Gaussian codebook for quantizing each KL coefficient. However, the symmetry around the reference antenna in uniform linear arrays allows generating the CQ codebook for one antenna from its symmetric counterpart. Moreover, the CQ codebooks can be stored in tables based on the tabulated correlation coefficient so that channel fading coefficients can be directly quantized from these tables.

In the simulation, the suburban macrocell scenario of the SCM has been considered [20]. The system consists of a BS equipped with N antennas, an adjacent antenna separation of d meters, several single antenna MSs moving at $v_{\mathrm{MS}} = 40$ km/h, and a carrier frequency of $f_c = 2$ GHz. The effects of path loss and shadowing have not been considered. Since the SCM does not specify the spatial correlation explicitly, the correlation estimation has been performed using the maximum likelihood estimator over segments of 40 ms, as detailed in [31]. The parameter L_{ch} is set to 10, which is one of the possible values detailed in [29]. Uniform quantization is used to quantize the correlation coefficients using $B_{\mathrm{cc}} = 5$ bits, which is a reasonable value according to [32].

Figs. 7-9 compare the performance of the PQ, KL, and CQ schemes regarding the estimated MSE per antenna, obtained through Monte Carlo simulations for different number of quantization bits. The estimated MSE per antenna can be expressed as

$$\mathrm{MSE} \approx \frac{1}{KN} \sum_{k=1}^{K} \|\mathbf{h}_k - \hat{\mathbf{h}}_k\|^2, \tag{44}$$

where $K = 10^5$ is the number of channel realizations in the simulation and $\mathbf{h}_k$ and $\hat{\mathbf{h}}_k$ are the original and the quantized channel, respectively, for the kth channel realization. While the PQ scheme uses all the bits to quantize the instantaneous CSI, the KL and CQ schemes dedicate some bits to quantizing the correlation coefficients. In order to make a fair comparison, the sum of bits dedicated to quantizing the instantaneous CSI and those dedicated to quantizing the correlation information during L_{ch} quantization processes is the same for the three schemes. Thus, the horizontal axis in the three figures shows the average number of bits per channel quantization.

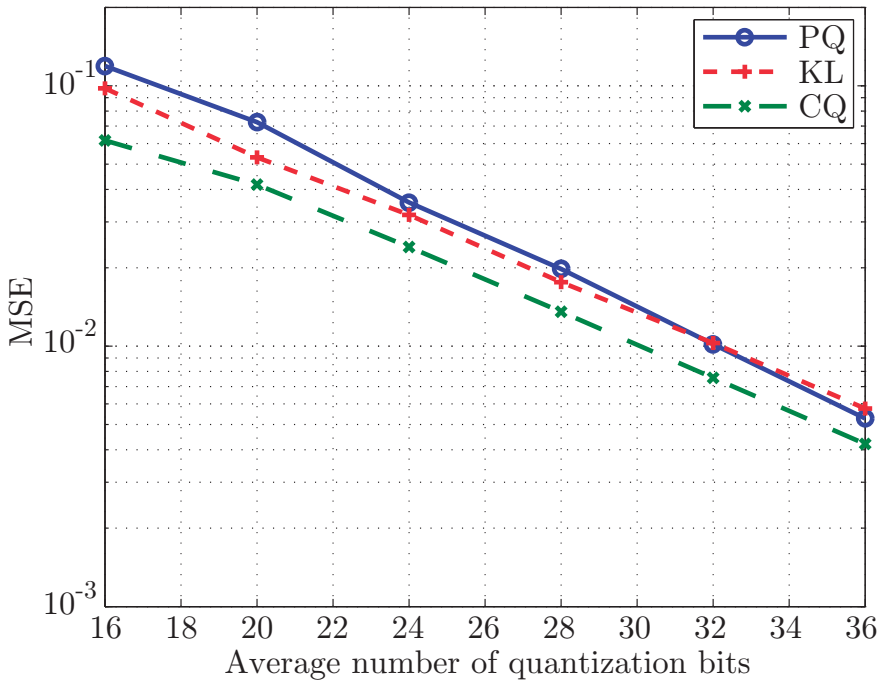

Fig. 7: MSE for $N = 4$, $d = \lambda/2$ and different average number of quantization bits.

Fig. 7 shows the MSE performance in a highly correlated scenario where the separation between two adjacent antennas of the array is set to $d = \lambda/2$. It can be observed that the CQ scheme outperforms the PQ and KL schemes, allowing a reduction of about $2-4$ quantization bits for a given MSE. Although the KL scheme is considered to be optimal in terms of decorrelation of Gaussian sources, it quantizes more correlation coefficients than the CQ scheme as seen in (42)-(43), which in turn results in fewer bits available to quantize the instantaneous CSI. In addition, the KL scheme presents a higher sensitivity to estimation and quantization errors in the correlation coefficients than the CQ scheme. This drawback could be solved by increasing B_{cc}, but it entails a reduction in the number of bits dedicated to quantizing the instantaneous CSI, obtaining a similar performance (the results with $B_{\text{cc}} = 8$ are omitted since a very similar performance to that shown for $B_{\text{cc}} = 5$ is obtained). The choice of the optimal B_{cc} may depend on the value of L_{ch} since a longer validity period can be advantageous in order to provide more accurate correlation information, however, this analysis is out of the scope of this paper.

In Fig. 8, the adjacent antenna separation is set to $d = \lambda$. Consequently, the correlation of the transmit antennas decreases and so does the difference between the performance of the CQ

scheme and the PQ scheme. However, the CQ scheme still outperforms the PQ scheme in almost the entire considered range. The poor performance obtained by the KL scheme can be explained by the considerable number of feedback bits that are used to quantize the correlation coefficients, whereas the correlation is not as high in Fig. 8 as in Fig. 7.

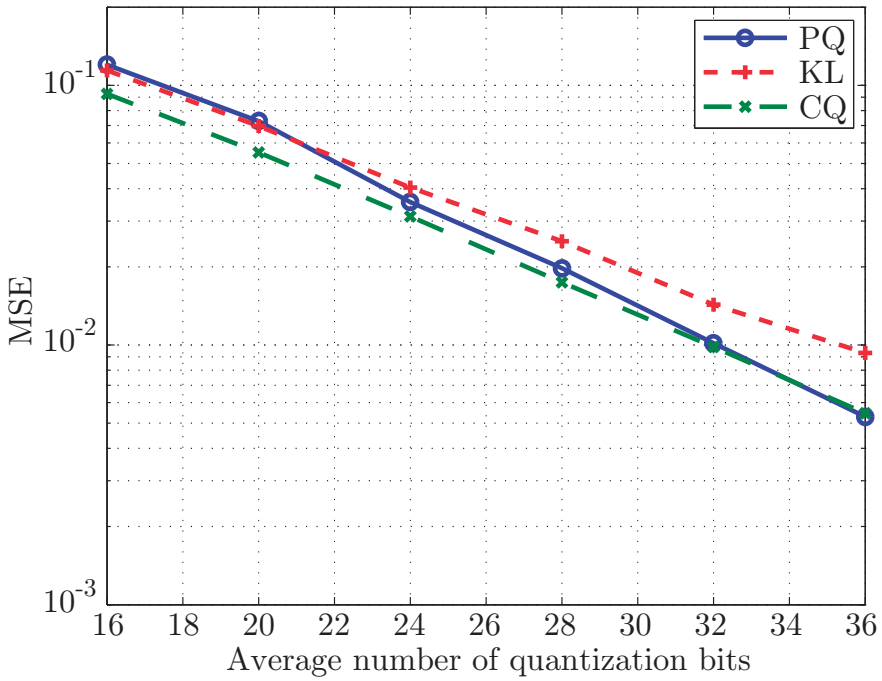

Fig. 8: MSE for $N = 4$, $d = \lambda$ and different average number of quantization bits.

Fig. 9 shows the MSE performance for a system with $N = 8$ transmit antennas and $d = \lambda/2$. It is important to note that, even though the antenna separation is as small as in Fig. 7, the distance between non-adjacent antennas increases with the number of antennas and the correlation between non-adjacent antennas decreases. In this case, the CQ scheme outperforms the PQ and KL schemes, but the differences between the PQ scheme and the CQ scheme are not as relevant. The KL scheme has to quantize $N_{\mathrm{c,KL}} = 28$ correlation coefficients, whereas CQ only has to quantize $N_{\mathrm{c,CQ}} = 7$. Thus, CQ can use more bits to quantize the instantaneous CSI and performs better over the entire range of bits.

Fig. 10 shows the MSE of the different schemes in terms of the adjacent antenna separation, d, for $N = 4$ antennas and an average number of 28 quantization bits, whereas Fig. 11 shows the MSE for $N = 8$ antennas and an average number of 56 quantization bits. Note

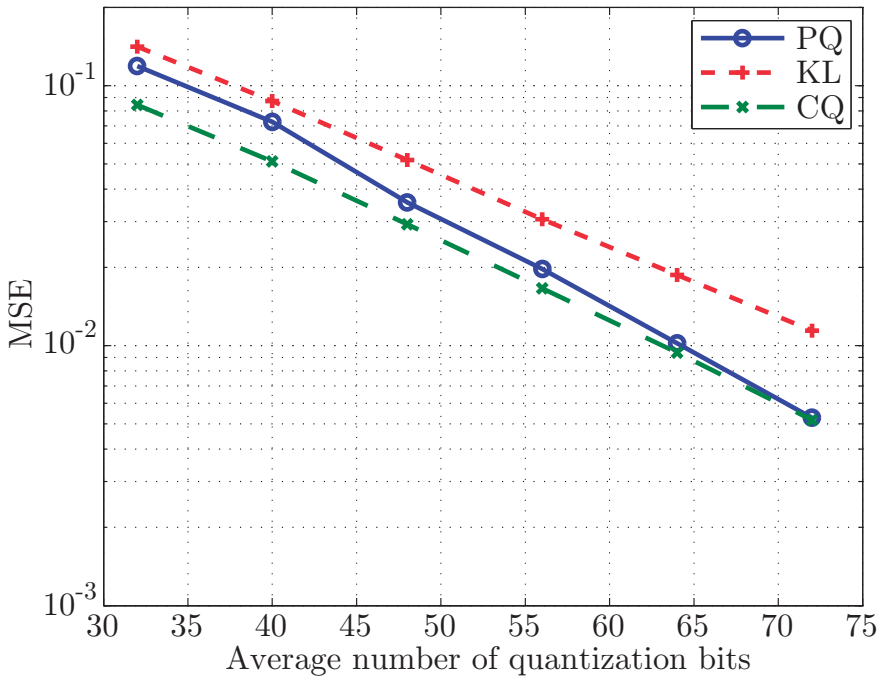

Fig. 9: MSE for $N = 8$, $d = \lambda/2$ and different average number of quantization bits.

that spatial correlation together with the statistical characterization of the respective fading can be successfully used to reduce the MSE in the quantization of a MIMO channel in highly correlated environments, corresponding to arrays with close antennas. In our simulated systems, the correlation could be exploited by the CQ scheme to obtain the best performance for antenna separations below $d = 1.3\lambda$ and $d = 0.75\lambda$ for the cases of $N = 4$ and $N = 8$ antennas, respectively. It is important to note that the CQ scheme is equivalent to the PQ scheme when the correlation is not considered, although this case has not been contemplated in the simulations. Thus, the MSs would hypothetically choose whether or not to provide the correlation information, assuming the BS that $\rho = 0$ when the information is not provided, and achieving the best performance between CQ and PQ for each case. Similarly, the KL scheme is equivalent to rectangular quantization when the correlation is not considered and its performance is almost identical to the PQ scheme [13].

V. Conclusion

A spatial statistical characterization of the channel in a system with multiple transmit antennas has been presented in this work. In this characterization, one antenna is selected as the reference

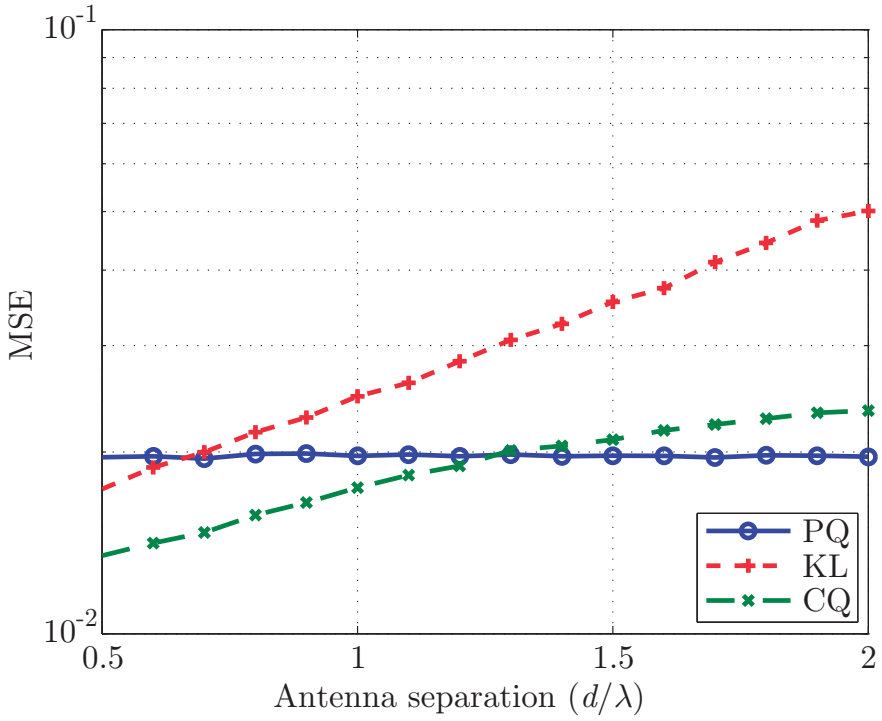

Fig. 10: MSE for $N = 4$, different antenna separations and an average number of quantization bits of 28 bits.

antenna and the channel fading from this antenna is considered to be the reference channel fading. The statistics for the fading of the rest of the channels are stated and related to the reference fading by means of the correlation coefficient. The envelope of a non-reference channel fading is characterized using the conditional probability density function given the envelope of the reference channel fading and the correlation coefficient of the non-reference channel fading with the reference fading. The phase of a non-reference channel fading is characterized by using an approximation that is based on high correlation and the statistical characterization of the error that is induced by this approximation.

A new channel quantization scheme that makes use of this characterization to reduce the feedback information has also been proposed. In this scheme, the envelope and the phase of the reference channel fading are quantized considering a Rayleigh distribution and a uniform distribution, respectively. The envelopes of the non-reference channel fading coefficients are quantized according to their conditional probability density function given the reference channel fading

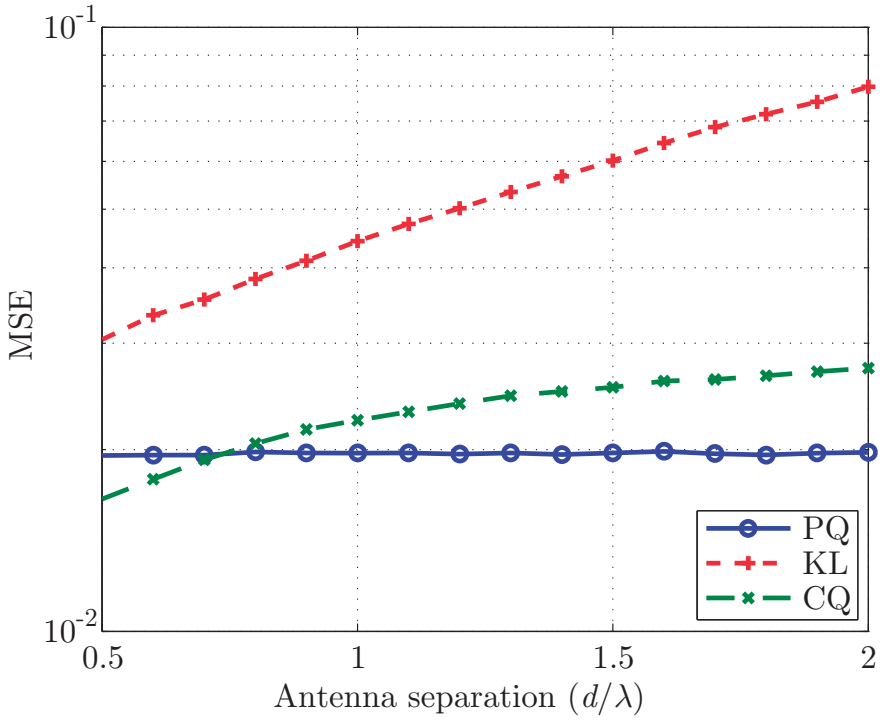

Fig. 11: MSE for $N = 8$, different antenna separations and an average number of quantization bits of 56 bits.

envelope and the correlation coefficient. Finally, the phase of the non-reference channel fading is fed back by quantizing the error of its approximation using the proposed characterization.

The proposed scheme has been compared with a scheme that is based on standard polar quantization where the spatial correlation is not taken into account, and a scheme based on the Karhunen-Loève transform, which achieves maximum decorrelation of Gaussian sources. The main advantage of the proposed scheme is that, unlike the scheme based on the Karhunen-Loève transform, it does not require the entire spatial correlation matrix. Thus, fewer feedback bits are used to quantize the correlation information and more bits are available to quantize the instantaneous CSI. The comparison has been carried out using the 3GPP spatial channel model (SCM). The numerical results show that the proposed scheme clearly outperforms the other two schemes in highly correlated scenarios. For the particular parameters used in our simulations, the proposed scheme allows the spatial correlation to be successfully exploited in arrays with adjacent antenna separations that are lower than $d = 1.3\lambda$ and $d = 0.75\lambda$ for $N = 4$ and $N = 8$

antennas, respectively. In addition, this scheme can be straightforwardly adapted to ignore the correlation when no benefit is obtained from it.

APPENDIX
DETAILS OF CALCULATIONS

The distortion in non-reference fading that is seen in (32) can be calculated by making use of the following results. For the conditional probability distribution $f(r_1|r_2)$, $m_n^{a,b}$ is defined as

$$\begin{aligned} m_n^{a,b}(r_{\rm r},\rho) &= \int_a^b r_{\rm nr}^n f(r_{\rm nr}|r_{\rm r}){\rm d}r_{\rm nr} = \\ &= \int_a^b \frac{r_{\rm nr}^{n+1}}{b^2(1-|p|^2)} \exp\left(-\frac{r_{\rm nr}^2+r_{\rm r}^2|p|^2}{2b^2(1-|p|^2)}\right) \sum_{k=0}^{\infty} \frac{\left(r_{\rm nr}r_{\rm r}|p|\right)^{2k}}{\left(2b^2(1-|p|^2)\right)^{2k}(k!)^2}{\rm d}r_{\rm nr}, \end{aligned} \tag{45}$$

where the Taylor series expansion around $x=0$ of the modified Bessel function of the first kind with order 0 has been used [25, Sec. 9],

$$I_0(x) = \sum_{k=0}^{\infty} \frac{x^{2k}}{2^{2k}(k!)^2}. \tag{46}$$

Defining $A = 2b^2(1-|p|^2)$, $C = r_{\rm r}^2|p|^2$ and using a change of variables $t = r_{\rm nr}^2/A$, we can express $m_n^{a,b}(r_{\rm r},\rho)$ as

$$m_n^{a,b}(r_{\rm r},\rho) = \exp\left(\frac{-C}{A}\right) \sum_{k=0}^{\infty} \frac{C^k\left(\Gamma\left(k+\frac{n}{2}+1,\frac{a^2}{A}\right)-\Gamma\left(k+\frac{n}{2}+1,\frac{b^2}{A}\right)\right)}{A^{k-\frac{n}{2}}(k!)^2}, \tag{47}$$

where $\Gamma(s,x)$ denotes the upper incomplete Gamma function [25, Sec. 6]. When $a=0$ and $b\to\infty$, $m_n^{a,b}(r_{\rm r},\rho)$ becomes the moment taken about 0, also known as raw moment, which has been expressed in (16).

The following result, which is related to the phase deviation Δ, also appears as a part of (32) and can be obtained through an integration by parts:

$$\begin{aligned} \int_{\Delta_{p-1}}^{\Delta_p} \cos(\Delta-\hat{\Delta}_p)\tilde{f}_{\Delta}(\Delta,\rho){\rm d}\Delta = &\frac{1}{2(1-\exp(-\pi/b_{\rm L}))(1+b_{\rm L}^2)}\Big[\left(\mathrm{sgn}(\Delta_p)-\mathrm{sgn}(\Delta_{p-1})\right)\cos(\hat{\Delta}_p) \\ &-\exp\left(\frac{-|\Delta_{p-1}|}{b_{\rm L}}\right)\Big(b\sin(\Delta_{p-1}-\hat{\Delta}_p)-\mathrm{sgn}(\Delta_{p-1})\cos(\Delta_{p-1}-\hat{\Delta}_p)\Big) \\ &+\exp\left(\frac{-|\Delta_p|}{b_{\rm L}}\right)\Big(b\sin(\Delta_p-\hat{\Delta}_p)-\mathrm{sgn}(\Delta_p)\cos(\Delta_p-\hat{\Delta}_p)\Big)\Big], \end{aligned} \tag{48}$$

where $b_{\rm L}$ is given by (34).

REFERENCES

[1] A. J. Paulraj, D. A. Gore, R. U. Nabar, and H. Bolcskei, "An overview of MIMO communications - a key to gigabit wireless," *Proceedings of the IEEE*, vol. 92, no. 2, pp. 198–218, 2004.

[2] A. Goldsmith, S. A. Jafar, N. Jindal, and S. Vishwanath, "Capacity limits of MIMO channels," *IEEE J. Sel. Areas Commun.*, vol. 21, no. 5, pp. 684–702, 2003.

[3] G. Caire and S. Shamai, "On the achievable throughput of a multiantenna Gaussian broadcast channel," *IEEE Trans. Inf. Theory*, vol. 49, no. 7, pp. 1691–1706, 2003.

[4] D. Gesbert, M. Kountouris, R. W. Heath, C.-B. Chae, and T. Salzer, "Shifting the MIMO paradigm," *IEEE Signal Process. Mag.*, vol. 24, no. 5, pp. 36–46, 2007.

[5] D. J. Love, R. W. Heath, V. K. N. Lau, D. Gesbert, B. D. Rao, and M. Andrews, "An overview of limited feedback in wireless communication systems," *IEEE J. Sel. Areas Commun.*, vol. 26, no. 8, pp. 1341–1365, 2008.

[6] J. Choi and R. W. Heath, Jr., "Interpolation based transmit beamforming for MIMO-OFDM with limited feedback," *IEEE Trans. Signal Process.*, vol. 53, no. 11, pp. 4125–4135, 2005.

[7] J. Choi, B. Mondal, and R. W. Heath, "Interpolation based unitary precoding for spatial multiplexing MIMO-OFDM with limited feedback," *IEEE Trans. Signal Process.*, vol. 54, no. 12, pp. 4730–4740, 2006.

[8] B. Mondal and R. W. Heath, "Channel adaptive quantization for limited feedback MIMO beamforming systems," *IEEE Trans. Signal Process.*, vol. 54, no. 12, pp. 4717–4729, 2006.

[9] V. Raghavan, R. W. Heath, and A. V. Sayeed M., "Systematic codebook designs for quantized beamforming in correlated MIMO channels," *IEEE J. Sel. Areas Commun.*, vol. 25, no. 7, pp. 1298–1310, 2007.

[10] T. Yoo, N. Jindal, and A. Goldsmith, "Multi-antenna downlink channels with limited feedback and user selection," *IEEE J. Sel. Areas Commun.*, vol. 25, no. 7, pp. 1478–1491, 2007.

[11] M. Trivellato, S. Tomasin, and N. Benvenuto, "On channel quantization and feedback strategies for multiuser MIMO-OFDM downlink systems," *IEEE Trans. Commun.*, vol. 57, no. 9, pp. 2645–2654, 2009.

[12] H. Shirani-Mehr and G. Caire, "Channel state feedback schemes for multiuser MIMO-

OFDM downlink," *IEEE Trans. Commun.*, vol. 57, no. 9, pp. 2713–2723, 2009.

[13] J. Max, "Quantizing for minimum distortion," *IRE Transactions on Information Theory*, vol. 6, no. 1, pp. 7–12, 1960.

[14] W. Pearlman, "Polar quantization of a complex Gaussian random variable," *IEEE Trans. Commun.*, vol. 27, no. 6, pp. 892–899, 1979.

[15] A. Gersho and R. M. Gray, *Vector quantization and signal compression*. Norwell, MA, USA: Kluwer Academic Publishers, 1991.

[16] P. Castro, M. Joham, L. Castedo, and W. Utschick, "Robust precoding for multi-user MISO systems with limited-feedback channels," in *Proceedings of the International ITG Workshop on Smart Antennas*, Vienna, Austria, 2007.

[17] M. Nakagawa and M. Miyahara, "Generalized Karhunen-Loeve transformation I (theoretical consideration)," *IEEE Trans. Commun.*, vol. 35, no. 2, pp. 215–223, 1987.

[18] D.-S. Shiu, G. J. Foschini, M. J. Gans, and J. M. Kahn, "Fading correlation and its effect on the capacity of multielement antenna systems," *IEEE Trans. Commun.*, vol. 48, no. 3, pp. 502–513, 2000.

[19] C.-N. Chuah, D. Tse, J. Kahn, and R. Valenzuela, "Capacity scaling in MIMO wireless systems under correlated fading," *IEEE Trans. Inf. Theory*, vol. 48, no. 3, pp. 637–650, 2002.

[20] 3GPP TR 25.996 V10.0.0, "Spatial channel model for multiple input multiple output (MIMO) simulations."

[21] M. Simon and M. Alouini, *Digital Communication over Fading Channels*, ser. Wiley Series in Telecommunications and Signal Processing. Wiley-Interscience, 2005.

[22] C. Polprasert and J. Ritcey, "A Nakagami fading phase difference distribution and its impact on BER performance," *IEEE Trans. Wireless Commun.*, vol. 7, no. 7, pp. 2805–2813, 2008.

[23] A. Forenza, D. J. Love, and R. W. Heath, "Simplified spatial correlation models for clustered MIMO channels with different array configurations," *IEEE Trans. Veh. Technol.*, vol. 56, no. 4, pp. 1924–1934, 2007.

[24] V. Raghavan, J. H. Kotecha, and A. Sayeed, "Why does the kronecker model result in misleading capacity estimates?" *IEEE Trans. Inf. Theory*, vol. 56, no. 10, pp. 4843–4864, 2010.

[25] M. Abramowitz and I. A. Stegun, *Handbook of Mathematical Functions, With Formulas,*

Graphs, and Mathematical Tables. Dover Publications, Incorporated, 1974.

[26] V. Aalo, G. Efthymoglou, and C. Chayawan, "On the envelope and phase distributions for correlated gaussian quadratures," *IEEE Commun. Lett.*, vol. 11, no. 12, pp. 985–987, 2007.

[27] J. Lagarias, J. Reeds, M. Wright, and P. Wright, "Convergence properties of the Nelder–Mead simplex method in low dimensions," *SIAM Journal on Optimization*, vol. 9, no. 1, pp. 112 –147, 1998.

[28] R. A. Horn and C. R. Johnson, *Matrix Analysis*. Cambridge University Press, 2012.

[29] 3GPP TR 36.213 V11.4.0, "Physical layer procedures (Release 11)."

[30] S. Sesia, I. Toufik, and M. Baker, *LTE, The UMTS Long Term Evolution: From Theory to Practice*, 2nd ed. Wiley, 2011.

[31] T. J. Willink, "Limits on estimating autocorrelation matrices from mobile mimo measurements," *International Journal of Antennas and Propagation*, vol. 2013, p. 6 pages, 2013.

[32] S. Ghosh, B. Rao, and J. Zeidler, "Techniques for MIMO channel covariance matrix quantization," *IEEE Trans. Signal Process.*, vol. 60, no. 6, pp. 3340–3345, 2012.